BBA - Gene Regulatory Mechanisms 1862 (2019) 509–521

Contents lists available at ScienceDirect

BBA - Gene Regulatory Mechanisms

journal homepage: www.elsevier.com/locate/bbagrm

The complex CBX7-PRMT1 has a critical role in regulating *E-cadherin* gene expression and cell migration

Antonella Federico[a], Romina Sepe[a], Flora Cozzolino[b], Claudia Piccolo[a], Carla Iannone[b], Ilaria Iacobucci[b], Piero Pucci[b], Maria Monti[b], Alfredo Fusco[a,*]

[a] Istituto di Endocrinologia ed Oncologia Sperimentale - CNR c/o Dipartimento di Medicina Molecolare e Biotecnologie Mediche, Università degli Studi di Napoli "Federico II", Naples, Italy
[b] Dipartimento di Scienze Chimiche, Università degli Studi di Napoli "Federico II" and CEINGE Biotecnologie Avanzate, Napoli, Italy

ARTICLE INFO

Keywords:
CBX7
PRMT1
E-cadherin
Cell migration
Cancer progression

ABSTRACT

The Chromobox protein homolog 7 (CBX7) belongs to the Polycomb Group (PcG) family, and, as part of the Polycomb repressive complex (PRC1), contributes to maintain transcriptional gene repression. Loss of CBX7 expression has been reported in several human malignant neoplasias, where it often correlates with an advanced cancer state and poor survival, proposing CBX7 as a candidate tumor-suppressor gene in cancer progression. Indeed, CBX7 is able to positively or negatively regulate the expression of genes involved in cell proliferation and cancer progression, such as *E-cadherin*, *cyclin E*, *osteopontin*, *EGR1*.

To understand the molecular mechanisms that underlie the involvement of CBX7 in cancer progression, we designed a functional proteomic experiment based on CHIP-MS to identify novel CBX7 protein partners. Among the identified CBX7-interacting proteins we focused our attention on the Protein Arginine Methyltransferase 1 (PRMT1) whose critical role in epithelial-mesenchymal transition (EMT), cancer cell migration and invasion has been already reported. We confirmed the interaction between CBX7 and PRMT1 and demonstrated that this interaction is crucial for PRMT1 enzymatic activity both *in vitro* and *in vivo* and for the regulation of *E-cadherin* expression, an important hallmark of EMT.

These results suggest a general mechanism by which CBX7 interacting with histone modification enzymes like HDAC2 and PRMT1 enhances *E-cadherin* expression. Therefore, disruption of this equilibrium may induce impairment of *E-cadherin* expression and increased cell migration eventually leading to EMT and, then, cancer progression.

1. Introduction

Polycomb group (PcG) proteins are a class of structurally diverse but functionally related epigenetic regulators involved in morphogenesis, chromosome X-inactivation, haematopoiesis, stem-cell self-renewal, cellular proliferation, senescence and tumorigenesis [1–3]. Biochemical and genetic studies indicate that PcG proteins act as part of two major multiprotein complexes referred as the Polycomb repressive complexes 1 and 2 (PRC1 and PRC2) that contribute to gene repression by inhibiting transcription initiation [4].

CBX7 (chromobox homolog 7), a component of the PRC1 complex, belongs to a mammalian family of chromobox-containing proteins with its amino-terminal region, between amino acids 10 and 46, containing a "CHROMO" domain (*Chromatin Organization Modifier Domain*, CD) that binds methyl-lysine residues [5]. Several studies report a reduced expression of CBX7 in different malignant neoplasias, such as thyroid [6], colorectal [7], pancreatic [8], bladder [9], gastric [10], lung [11], gliomas [12] and breast [13] carcinomas. Decreased CBX7 expression is associated to a more aggressive phenotype and reduced survival, indicating CBX7 as a candidate tumor-suppressor gene [14]. This role of CBX7 in carcinogenesis was confirmed by the generation of *Cbx7* knockout mice (KO). Indeed, both heterozygous $Cbx7^{+/-}$ and homozygous $Cbx7^{-/-}$ mice developed liver and lung adenomas and carcinomas [7]. Accordingly, MEFs derived from *Cbx7*-KO mice have a faster proliferation rate with higher number of cells in S phase than wt MEFs suggesting that *Cbx7* negatively regulates G_1/S transition [7].

Some of the mechanisms by which the lower expression of CBX7 contributes to cancer progression have already been unveiled. CBX7

* Corresponding author at: Dipartimento di Medicina Molecolare e Biotecnologie Mediche, Università degli Studi di Napoli "Federico II", Via Pansini 5, 80131 Naples, Italy.
E-mail address: alfusco@unina.it (A. Fusco).

https://doi.org/10.1016/j.bbagrm.2019.02.006
Received 24 May 2018; Received in revised form 19 February 2019; Accepted 25 February 2019
Available online 28 February 2019
1874-9399/

negatively regulates the expression of *CCNE1*, the gene coding for cyclin E, a regulator of cell cycle crucial for the G_1/S transition, counteracting the positive regulation exerted by HMGA1 proteins [7,11], and thereby modulating cell proliferation. By a very similar mechanism, CBX7 also negatively modulates the expression of *SPP1* gene encoding the osteopontin protein, a chemokine promoting cell migration and, then, associated with cancer progression [15,16].

Furthermore, it was reported that CBX7 positively regulates *E-cadherin* gene (*CDH1*) expression through the interaction with histone deacetylase 2 (HDAC2) [17]. Indeed, CBX7 physically interacts with HDAC2 and reduces its negative activity on the *CDH1* promoter, then positively regulating the expression of the *CDH1* gene [17]. It is noteworthy that *CDH1* is one of the caretaker genes of the normal epithelial phenotype and the loss of its expression leads to the critical event of the epithelial-to-mesenchymal transition (EMT). More recently, it was also reported that the restoration of CBX7 expression increases the susceptibility of human lung carcinoma cells to irinotecan treatment [18].

On this ground, we envisaged the hypothesis that CBX7 counteracts cancer progression also interacting with other proteins, thereby regulating the expression of other cancer-related genes. A comprehensive investigation of CBX7 biological functions was performed by functional proteomic experiments using a CHIP-MS based approach to immunoprecipitate V5-tagged CBX7 with the aim to identify new potential CBX7-interacting candidate proteins [19,20]. Among several CBX7 protein partners, we focused our attention on the prevalent protein arginine methyltransferase 1 (PRMT1). Indeed, several studies underline a critical role for PRMT1 deregulation in cancer since its overexpression has been described in several carcinomas including colon [21], breast [22], bladder [23], head and neck [24], lung, acute myeloid leukemia and mixed lineage leukemia [25,26]. Proteins belonging to PRMTs group are able to transfer methyl groups from the ubiquitous cofactor *S*-adenosyl-L-methionine (AdoMet) to the arginine residues of many histones and nuclear/cytoplasmic proteins. In particular, PRMT1 catalyzes the formation of H4R3me2a and H2AR11me1 on the histone proteins with a significant preference for arginine residues flanked by one or more glycine residues [26–29]. Epigenetic regulation is fundamental to the dynamic control-balance between stability and reversibility in gene expression projects. Post-translational modification of histones by methylation is an essential and common type of chromatin modification that is known to influence biological processes in the context of development and cellular responses. However, it is a crucial point that histone marks have context-dependent functions on transcription. In fact, there are examples where the same modifications can be associated with opposing effects on transcription [30].

We confirmed the interaction between CBX7 and PRMT1 by co-immunoprecipitation and demonstrated that this interaction occurred at the *CDH1* promoter, being crucial for regulating both PRMT1 enzymatic activity and *CDH1* expression. Indeed, we were able to demonstrate that CBX7 decreases the catalytic activity of PRMT1 at Arg3 of Histone H4 both *in vitro* and on the *CDH1* promoter. These data suggest that CBX7 contribute to the transcription of *CDH1* also by interacting with the mehyltransferase and impairing enzymatic activity of PRMT1.

2. Materials and methods

2.1. Cell culture, vector and transfection

HEK293 cell line was grown in DMEM (Life Technologies, Grand Island, NY), instead A549 and HeLa in RPMI (Life Technologies). Both medium were supplemented with 10% fetal bovine serum, 1% L-glutamine 10 mM, 1% penicillin/streptomycin (Life Technologies). All cell lines were maintained at 37 °C under 5% CO2 atmosphere.

HeLa cells were transfected by using Fugene HD reagent (Promega, Fitchburg, WI), while the Neon Electroporation System (Life Technologies) was used for the HEK293 cells, and LIPO2000 (Life Technologies) for A549 clones (EV4, C2 and C4), according to manufacturer's instructions.

The expression vectors encoding the CBX7 protein fused to V5 or HA epitope (V5-CBX7 or HA-CBX7) have been previously described [17]. The vector expressing the PRMT1 protein was provided by Genecopoeia™ (MYC-tagget-PRMT1). GST fusion proteins were constructed by cloning the human cDNA sequence of *CBX7* in a pGEX4T-1 vector (Promega) as previously described [17]. For all transfections, the total amount of the transfected DNA was balanced with the empty vector.

2.2. Luciferase assays

1.5×10^5 HeLa cells were seeded in 6-well plate, transfected with 50 ng of the *CDH1*- luciferase reporter gene and expression vectors encoding the CBX7 and PRMT1 proteins. 48 h after transfection, cell extracts were prepared and the luciferase activity was measured by using a Lumat LB9507 luminometer (Berthold Technologies, Bad Wildbad, Germany) and the Dual-Luciferase Reporter System kit (Promega). A vector expressing *Renilla* gene under the control of the cytomegalovirus (CMV) promoter was used to normalize transfection efficiency. For all transfections, the total amount of the transfected DNA was balanced with the empty vector.

2.3. RNA extraction and quantitative RT-qPCR

Total RNA was extracted from cell lines by using Trizol reagent (Life Technologies), according to manufacturer's instructions. 1 μg of total RNA was used to obtain the cDNA with the QuantiTect Reverse Transcription Kit (Qiagen). RT-qPCR analysis was carried out in 96-well plates with the CFX 96 thermocycler (Bio- Rad, Hercules, CA) by using 20 ng of each cDNA and Sybr Green (Applied Biosystems, Foster City, CA). Detailed primer sequences are available as Supplementary Materials and Methods. Relative Expression was calculated according to the $2^{-\Delta\Delta Ct}$ formula and expression value of controls was set equal to 1 [31].

2.4. Protein extraction, Western blot analysis, immunoprecipitation and GST pull down experiments

Total protein extracts were obtained by using the JS lysis buffer (20 mM Tris-HCl pH 7.5, 5 mM EDTA, 150 mM NaCl, 1% Nonidet P40) completed with a mix of inhibitors of proteases and phosphatases. The extracted proteins were separated by SDS-PAGE and then transferred onto Protran membranes (Perkin Elmer, Boston, MA). Membranes were blocked with BSA or 5% non-fat milk and then incubated with the following antibodies: anti-V5 (Invitrogen, Carlsband, CA, R960), anti-MYC tag (Abcam, ab9132; Millipore 05-724), anti-PRMT1 (Millipore, 07–404), anti- γ-vinculin (Santa Cruz, sc-7649), anti-GAPDH (Santa cruz, sc-32233), anti-α-Tubulin (Sigma, T5168), anti-γ-Tubulin (Santa cruz, sc-17787). Membranes were then incubated with horseradish peroxidase-conjugated secondary antibody (1:3000) for 60 min at room temperature and the signals were detected by enhanced chemiluminescence (ECL) detection system (Thermo Fisher Scientific, Inc., Waltham, MA). Immunoprecipitation (IP) procedures were carried out as reported elsewhere [17]. Antibodies used for IP with untransfected cells were anti-CBX7 (Abcam ab-21873), anti- PRMT1 (Millipore 07-404), for IP in transfected cells were anti-V5 (Abcam ab-1229), eluated by V5-peptide (Abcam ab-15829).

2.5. Chromatin immunoprecipitation and mass spectrometry (ChIP-MS) assays

ChIP-MS experiments (ChIP-MS) were performed in HEK293 cells, transiently transfected with V5-tagged CBX7 (V5-CBX7) and the same cell line transfected with an empty vector used as control [32,33]. Cells were incubated in 50 mM HEPES pH 7.5, 100 mM NaCl, 1 mM EDTA, 0.5 mM EGTA and formaldehyde at a final concentration of 0.75% at

room temperature for 20 min and the reaction was stopped by adding glycine at a final concentration of 0.125 M. The protein nuclear extracts were prepared as reported [32]. Briefly, cells were lysed by using a cytosolic buffer (50 mM HEPES pH 7.5, 140 mM NaCl, 1 mM EDTA, 10% glycerol, 0.5% NP-40, 0.25% Triton X100 and protease inhibitors), thus obtaining the cytosolic extracts that were discarded; the remaining pellets were washed in 10 mM Tris-Cl pH 8.0, 200 mM NaCl, 1 mM EDTA, 0 .5mM EGTA and protease inhibitors, and finally lysed in buffer containing 10 mM Tris-Cl pH 8.0, 10 mM NaCl, 1 mM EDTA, 0 .5mM EGTA, 0.1% Na-Deoxycholate, 0.5% N-laurylsarcosine and protease inhibitors, by sonicating several times for 10 min at maximum settings to obtain fragments between 400 and 600 bp. Then, Triton X-100 was added to sample and control up to a final concentration of 1%. The protein samples were pre-cleared by a o.n. incubation at 4 °C on protein A-magnetic beads (Life Technologies) previously treated with a Blocking Solution (1X PBS, 0.5% BSA w/v). The pre-cleared extracts were then imunoprecipitated with anti-V5 antibody (Ab15828 Abcam) and protein A-magnetic beads. Following washing steps, the elution of protein complex has been carried out contemporaneously to the de-cross linking process adding de-cross linking/elution buffer 1X (250mM Tris-HCl pH 8.8, 2% SDS, 0.5 M β mercaptoethanol) and incubating at 95 °C for 20 min. 4/5 in volume of final sample were employed for the proteomic assay while 1/5 for the PCR.

The protein samples for proteomics analysis were separated by SDS-PAGE and the gel was stained by colloidal blue comassie. Sample and control lanes were cut in 1 mm slices and the protein bands digested by trypsin as reported [20,34,35]. The peptide mixtures were then freeze-dried and re-suspended in 10 ml of 0.2% Formic Acid for the nanoLC-MS/MS analysis. Nano-Liquid Chromatography Tandem Mass Spectrometry (nanoLC-MS/MS) analyses were performed on a CHIP MS Ion Trap XCT Ultra equipped with a capillary 1100 HPLC system and a chip cube (Agilent Technologies, Palo Alto, CA). nanoLC-MS/MS raw data were employed for protein identification by using a licensed Mascot software (Matrix Science, Boston, USA) to search in database containing only human protein sequences [34,35].

2.6. ChIP and re-ChIP assays

ChIP and re-ChIP experiments were performed as reported elsewhere [11,17]. Briefly, 48 h after transfection, 5×10^6 HEK 293 cells were cross-linked to fix the DNA-protein complexes using 1% formaldehyde at room temperature for 10 min and the reaction was then stopped by adding glycine at a final concentration of 0.125 M. Cells were lysed in 300 µl of buffer containing 10 mM EDTA, 50 mM Tris-HCl pH 8.0, 1% SDS and protease inhibitors and then sonicated three times for 10 cycles (30′ ON, 30′ OFF) at maximum settings (BioruptorTM Next Gen, Diagenode Inc., Denville, NJ), obtaining fragments between 0.3 and 1.0 kb. After centrifuging samples at 14000 rpm for 15 min at 4 °C, 3% of supernatant amount was used as control of the total chromatin obtained (input), and the remaining part of the sample was diluted 2.5-fold in IP buffer (100 mM NaCl, 2 mM EDTA pH 8.0, 20 mM Tris-HCl pH 8.0, 0.5% Triton X-100 and protease inhibitors). After 3 h of pre-clearing at 4 °C with protein A- or protein G-Sepharose saturated with salmon sperm (Millipore, Billerica, MA), samples were mixed overnight at 4 °C with the following antibodies: anti-V5 (Ab15828 Abcam), anti-V5 (Sigma, V8137), anti-MYC tag (Abcam, ab9132), anti-H4R3me2a (Active motif, 39,705), anti-H3K27me3 (Millipore, 07–449), normal mouse IgG (sc-2025, Santa Cruz Biotechnology, Inc.), normal rabbit IgG (sc-2027, Santa Cruz Biotechnology, Inc.). Subsequently, the DNA-protein-antibodies complexes were immunoprecipitated with the proteins A/G previously used and then the chromatin was released from the beads through 30 min incubation with 250 µl of 1% SDS, 0.1 M NaHCO3 at 37 °C and finally with 200 nM NaCl at 65 °C overnight. Subsequently, 10 µl of 0.5 mM EDTA, 20 µl of 1 M Tris-HCl pH 6.5 and 20 µg of Proteinase K were added to the reaction tube and then the complexes were incubated for 1 h at 45 °C. DNA from chromatin immunoprecipitated was purified by phenol/chloroform extraction (Life Technologies) and precipitated by adding two volumes of ethanol and 0.1 M CH_3COONa.

IgG were used as non specific control and input DNA values were used to normalize the values from qChIP samples. The percentage of IP chromatin was calculated as $2^{-\Delta\Delta Ct}$. ΔCt is the difference between Ct (sample) and Ct (input), while ΔΔCt is the difference between ΔCt (sample) and ΔCt (mean value of IgG). So, the IgG are set equal to 1 [31,36,37]. This input sample represents the amount of chromatin used in the ChIP. By this method, signals obtained from the ChIP are subtracted by those obtained from an input sample. In our experiments 3% of starting chromatin is used as input. Raising 2 to the DCt power yielded the relative amount of PCR product. The relative abundance of immunoprecipitated chromatin was expressed as percentage of binding of interested promoter compared to the input. For Fig. 3C the representation the value of empty vector (immunoprecipitated by Ab) was set to 1 as mean value of all samples. All ChIP data were resulted by more independent experiments, and for each experiment qPCR assay was performed at least in triplicate. Detailed primer sequences are available as Supplementary Materials and Methods.

2.7. In vitro methylation assay

The methylation reaction was conducted in 40 ml of PBS buffer (Euroclone) for 60 min at 37 °C incubating recombinant PRMT1 (3 mg) with 4 mg of core histones (Millipore) in presence of 5 mM AdoMet (Sigma Aldrich) and 4 mg of GST-CBX7 (Abnova); the same reaction, carried out in absence of CBX7, constituted the control. The reactions were stopped by Laemli buffer addition and the samples were then fractionated by SDS-PAGE on a 15% gel. Protein bands corresponding to H4 histone were excised from the gel, destained with acetronitrile/ammonium bicarbonate 0 .1M and hydrolysed by trypsin for 2 h at 37 °C. The hydrolysis shorter time has been previously set up on H4 histone thus to control the proteolysis events at N-terminus domain, rich of basic residues, and to obtain longer peptides than those expected by an extensive tryptic hydrolysis [34,35].

Peptide mixtures were analyzed by LC-MS/MS on a LTQ-Orbitrap XL mass spectrometer (ThermoFisher Scientific) equipped with a nano-electrospray ion source and coupled with a nanoEasy-LC II capillary HPLC system (Proxeon Biosystem). Samples were injected onto a capillary chromatographic system consisting of a 2 cm length trapping column (C18, ID 100um, 5um) and a 10 cm C18 reverse phase silica capillary column (ID 75um, 3um) (ThermoFisher Scientific). A gradient of 125 min of acetonitrile eluents was used for separation (0.3 µL/min flow rate). MS analysis was performed with a resolution set to 30,000, and mass range from m/z 300 to 1800 Da. The five most intense peptides ions with 2, 3 and 4 charged residues were selected and fragmented in the ion trap. All MS/MS samples were analyzed using licensed Mascot software (Matrix Science) to search in a restricted database containing only chicken histone sequences. Searches were performed up to 9-missed cleavages, allowing Acetyl (Protein N-term) as fixed modification and Acetyl (K), Dimethyl (K), Dimethyl (R), Methyl (K), Methyl (R), Oxidation (M), as variable modifications.

2.8. Cell migration assay

Transwell motility assays were performed using 8 µm pore, 6.5 polycarbonate transwell filter (Corning Costar Corp., Cambridge, MA). 24 h after transfection, 2.5×10^4 A549 cells were suspended in 200 ml serum-free medium and seeded on the upper surface of the filters and allowed to migrate toward 300 ml of 10% FBS-containing medium in the bottom compartment. Moreover, 2.5×10^4 A549 cells were plated in a 96-well plate in triplicate and treated with CellTiter96 Aqueous One (Promega) to confirm that we used the same number of cells for each condition. After additional 24 h, transwell filters were washed three times with PBS at room temperature and cells migrated to the

underside of filter were fixed and stained with crystal violet solution (0.1% crystal violet, 20% methanol). Cells remaining on the upper surface were removed with a cotton swab. In order to exactly quantify crystal violet staining, samples were de-stained with 0.1% SDS in 300 ml of PBS, the absorbance of eluates were read at 595 nm in a microplate readers (LX 800, Universal Microplate Reader, Biotek, Winooski, VT) and then normalized with CellTiter values. Extracted RNA and protein were analyzed to evaluate the expression of the transfected vectors.

2.9. Statistical analysis

D'Agostino-Pearson or KS tests were used to evaluate the statistical distribution of samples, and the ANOVA (parametric or non-parametric) was used to identify statistical significance of the obtained data. For comparison of two groups unpaired *t*-test was used. In all the experiments, the significance was considered for $p < 0.05$ (*) or $p < 0.01$ (**). Data are reported as mean values ± standard error of mean (SEM) for multiple experiments, and as mean values ± standard deviation (SD) for single experiment.

3. Results

3.1. Identification of CBX7 interacting proteins and target genes

The organization and functions of CBX7-containing protein complexes were investigated by a Chromatin Immunoprecipitation assay coupled with mass spectrometry (ChIP-MS) [32,33]. This experiment allowed us to identify both the DNA regions specifically bound by the CBX7 complexes and the individual protein components effectively belonging to these complexes. ChIP-MS experiments were performed in HEK293 cells transiently transfected with V5-tagged CBX7 (V5-CBX7). The same cell line transfected with an empty vector was used as control.

Protein complexes were covalently linked to DNA sequences and immunoprecipitated by using antibodies against the V5 epitope. Samples were also immunoprecipitated with aspecific IgG antibodies as a control for the PCR-samples. The immunoprecipitated material comprising V5-CBX7 containing proteins-DNA complexes was employed for both Polymerase Chain Reaction (PCR) assay to verify the binding of CBX7 to the promoters of known target genes and for proteomic analyses to identify individual protein components.

The DNA fragments released by the immunocomplexes were analyzed by qPCR assay using specific primers for the human *E-cadherin (CDH1), cyclin E (CCNE1)* and *p16 (CDKN2A*) promoters, that have already been reported as CBX7 target genes. As shown in Fig. 1A, the amount of immunoprecipitated (IP) chromatin amplified by PCR was higher in the cells transfected with V5-CBX7 vector than in those transfected with the empty vector, confirming that CBX7 specifically binds to the *CDH1, p16* and *CCNE1* promoters [11,17].

The elution of protein components was carried out at the same time of the de-cross linking process, as described in Material and Methods section. The V5-CBX7 immunoprecipitated protein complexes and the corresponding control were fractionated onto a 4–12% gradient SDS-PAGE. The entire gel lanes were cut into slices and each gel slice was submitted to *in situ* tryptic digestion [34–36]. The resulting peptide mixtures were directly analyzed by liquid chromatography tandem mass spectrometry (LC-MS/MS) and identified by the MASCOT protein database search [34,35]. Proteins identified both in the control and in the sample lanes were discarded, whereas those proteins solely occurring in the V5-CBX7 transfected sample and absent in the control were considered as putative CBX7 interactors (Table 1). Among the putative CBX7 partners, several proteins involved in DNA- or RNA binding (PUF60, PRPF19, HNRNPD, PCBP1) and chromatin modification (HDAC2, PRMT1) were identified as well as the binding to HDAC2, that has already been reported [17,38].

Surprisingly, no other PRC1 components have been identified in the proteomic experiments except for the SCML2 subunit belonging to Polycomb family. However, in a different experiment, V5-CBX7 immunoprecipitated protein complexes were fractionated by ultracentrifugation on glycerol-gradient and the fractions positive for V5-CBX7 were submitted to protein identification (data not shown). A number of PRC1 components, but not PRMT1, has been identified among CBX7 interactors whereas when PRMT1 was present no PRC1 proteins were found suggesting that the interaction of PRMT1 with CBX7 might be independent from PRC1.

Among the putative CBX7 interacting candidates, we focused our attention on the Protein Arginine Methyltransferase 1 (PRMT1) because of the critical role of its deregulation in cancer [21–26]. Moreover, PRMT1 is known to catalyze the formation of H4R3me2a and H2AR11me1 on the histone proteins with methylation of H4R3 being highly related to tumor grade and used to predict cancer recurrence [27–29].

The interaction between endogenous CBX7 and PRMT1 was confirmed by co-immunoprecipitation experiments. Nuclear extracts from wild type HEK293 cells were precleared with IgG agarose and immunoprecipitated by using anti-CBX7 and anti-PRMT1 antibodies. Immunoprecipitation experiments were separated on SDS-PAGE and western blots were probed with anti-PRMT1 and anti-CBX7, respectively, confirming the interaction between PRMT1 and CBX7 proteins, as shown in Fig. 1B.

In addition, HEK293 cells were transiently transfected with V5-CBX7 and MYC-PRMT1 and total protein extracts were immunoprecipitated using anti-V5 antibody. Immunoprecipitated proteins were separated on SDS-PAGE and western blots were probed with anti-MYC and anti-V5 for detection of the co-immunoprecipitated PRMT1 protein to verify the interaction between CBX7 and PRMT1. The bands showing the electrophoretic mobility expected for MYC-PRMT1 and V5-CBX7 were clearly revealed by anti-MYC and anti-V5 antibody in the same lane (Fig. 1C), confirming the interaction between CBX7 and PRMT1.

The specificity of this interaction was confirmed by pull-down assays by incubating HEK293 total protein extracts either with a recombinant form of CBX7 fused to GST (GST-CBX7) immobilized onto glutathione-conjugated agarose beads or the GST protein alone as control. GST-CBX7 bound proteins were eluted by an excess of free glutathione. Fig. 1D shows the corresponding western blot analysis performed with anti-PRMT1 antibody where a strong band with the electrophoretic mobility of PRMT1 was clearly detected only in the sample incubated with GST-CBX7, thus confirming the interaction between PRMT1 and CBX7.

3.2. CBX7 interacts with PRMT1 on the E-cadherin promoter

To investigate whether the interaction between CBX7 and PRMT1 takes place on the *CDH1* promoters, we carried out chromatin immunoprecipitation (ChIP) experiments in HEK293 cells.

First, we validated the binding of endogenous CBX7 on specific DNA promoters. The DNA-protein complexes were fixed, subjected to preclearing with IgG and then immunoprecipitated by the anti-CBX7 antibody. Samples were also immunoprecipitated with aspecific IgG antibodies as a control. Chromatin was then released by the immunocomplexes and analyzed by qPCR assay using specific primers for the human *CDH1* and *CCNE1* promoter. As shown in Fig. 2A, the amount of immunoprecipitated chromatin amplified by qPCR was higher in the samples immunoprecipitated by using anti-CBX7 antibody than in the control confirming that endogenous CBX7 binds the *CDH1* and *CCNE1* promoters.

Second, we transiently transfected HEK293 cells with either individually V5-CBX7 or MYC-PRMT1 or both vectors (Fig. 2C). The DNA-protein complex from cells over expressing V5-CBX7 were fixed and then immunoprecipitated by using antibodies against the V5 epitope. Samples were also immunoprecipitated with aspecific IgG antibodies as

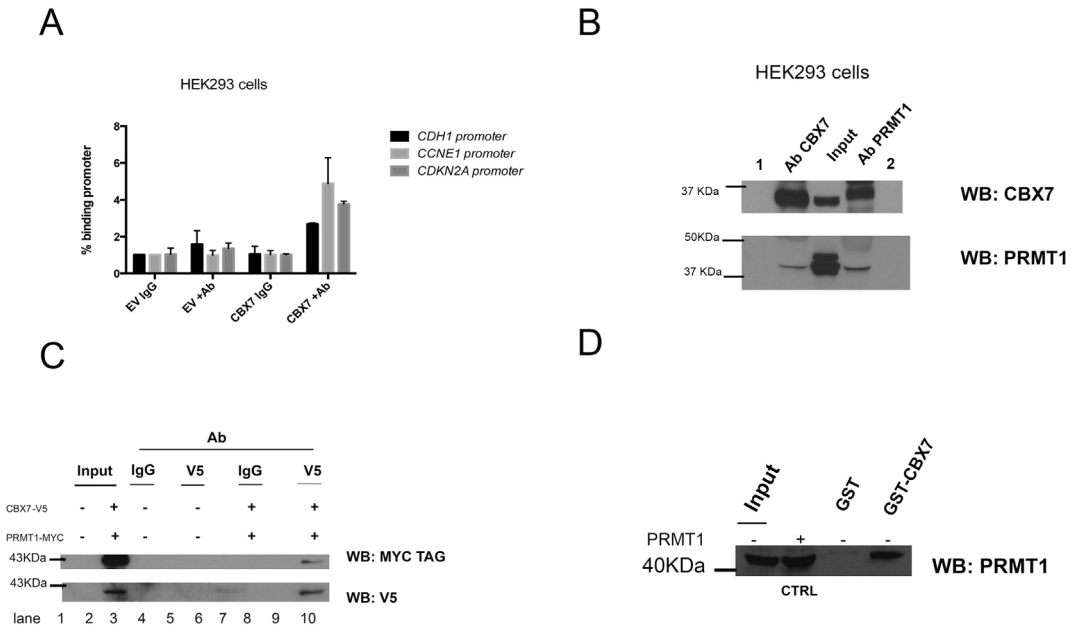

Fig. 1. CBX7 binds *CDH1, CCNE1* and *CDKN2A* promoters and interacts with PRMT1. A. HEK293 cells were transiently transfected with either a vector expressing V5-CBX7 (CBX7) protein or an empty vector (EV). The chromatin was immunoprecipitated by using antibodies (Ab) against the V5 epitope. IgG were used as negative control (IgG). The IP chromatin was analyzed by qPCR assay performed with primers specific for the *CDH1*, *CCNE1* and *CDKN2A* promoters. **B.** Nuclear extracts (NE) from HEK293 cells were subjected to pre-clearing (lane 1 and 2, respectively of Ab CBX7 and Ab PRMT1) and then immunoprecipitated with CBX7 antibody (Ab CBX7) and PRMT1 antibody (Ab PRMT1). Immunocomplexes were analyzed by Western blot with anti-CBX7 and anti-PRMT1 antibodies. Input: NE by HEK293 cells. **C.** HEK293 cells were transiently transfected with empty vector (lane 2) or V5-CBX7 and MYC-PRMT1 (lane 3) and co-immunoprecipitation experiments were carried out starting from total cellular extracts (TCE) by using anti-V5 antibodies (lane 6 and 10). IgG were used as an unrelated antibody (lane 4 and 8). Immunocomplexes were analyzed by Western blot with anti-MYC and anti-V5 antibodies. Input: TCE by cells transfected with empty vector (−) or V5-CBX7 and MYC-PRMT1 vector (+). **D.** GST pull-down assay was performed incubating HEK293 total cellular extracts either with GST or recombinant GST-CBX7 proteins. The filter was incubated with an anti-PRMT1 antibody. Input: TCE of HEK293 cells. CRTL: positive control expressing PRMT1 protein.

a control. Chromatin was then released by the immunocomplexes and analyzed by qPCR assay using specific primers for the human *CDH1* promoter. As shown in Fig. 2B the amount of immunoprecipitated chromatin amplified by qPCR was higher in the cells transfected with V5-CBX7 than in the control, as already reported [17].

Interestingly, when both V5CBX7 and MYC-PRMT1 were contemporaneously overexpressed (Fig. 2C), the amount of IP chromatin was lower than in the presence of CBX7 alone (Fig. 2B), indicating that the contemporary overexpression of CBX7 and PRMT1 decreases the binding of CBX7 to the *CDH1* promoter. These results indicate that the binding of CBX7 to CDH1 promoter is compromised by PRMT1 overexpression, thus suggesting a reduced interaction or accessibility for DNA binding when the proteins interact.

When HEK293 cells were transiently transfected with both V5-CBX7 and MYC-PRMT1 vectors, a ReChIP experiment was carried out by immunoprecipitating chromatin with anti-V5 first (Supplementary Figure 1) and then with anti-MYC antibodies. The results reported in Fig. 2D clearly indicated a large increase in the amount of immunoprecipitated chromatin amplified by qPCR following the ReChIP procedure demonstrating that the CBX7/PRMT1 interaction occurred at the *CDH1* promoter.

Finally, no amplification was observed when the chromatin was immunoprecipitated with anti-MYC antibodies in HEK293 over expressing MYC-PRMT1, indicating that PRMT1 alone was not able to bind the *CDH1* promoter (Fig. 2E).

3.3. H4R3 dimethylation is affected by CBX7 in vitro

PRMT1 is known to methylate Arg3 of histone H4 (H4R3) and this asymmetric dimethylation affects transcription [28–30]. However, the downstream consequences of the methylation event are poorly understood in many cases. Indeed, recent studies report that effects of methylation can be also context dependent [30].

To investigate the putative biological effect of the CBX7/PRMT1

Table 1
Proteins identifyed by CBX7/ChIP-MS.

Protein name (UniProt)	Gene	Peptides	MW (kDa)	UniProt code
Sex comb on midleg-like protein 2	SCML2	3	78	Q9UQR0
Exosome complex component RRP45	EXOSC9	5	40	Q06265
Poly(U)-binding-splicing factor PUF60	PUF60	5	58	Q9UHX1
Histone deacetylase 2	HDAC2	3	65	Q92769
T-complex protein 1 subunit theta	CCT8	5	60	P50990
Pre-mRNA-processing factor 19	PRPF19	3	56	Q9UMS4
Protein arginine *N*-methyltransferase 1	PRMT1	11	40	Q99873
Poly(rC)-binding protein 1	PCBP1	7	38	Q15365
Heterogeneous nuclear ribonucleoprotein D0	HNRNPD	3	36	Q14103
Chromobox protein homolog 7	**CBX7**	**9**	**28**	**O95931**
BTB/POZ domain-containing protein KCTD12	KCTD12	8	36	Q96CX2
Nucleophosmin	NPM1	3	31	P06748

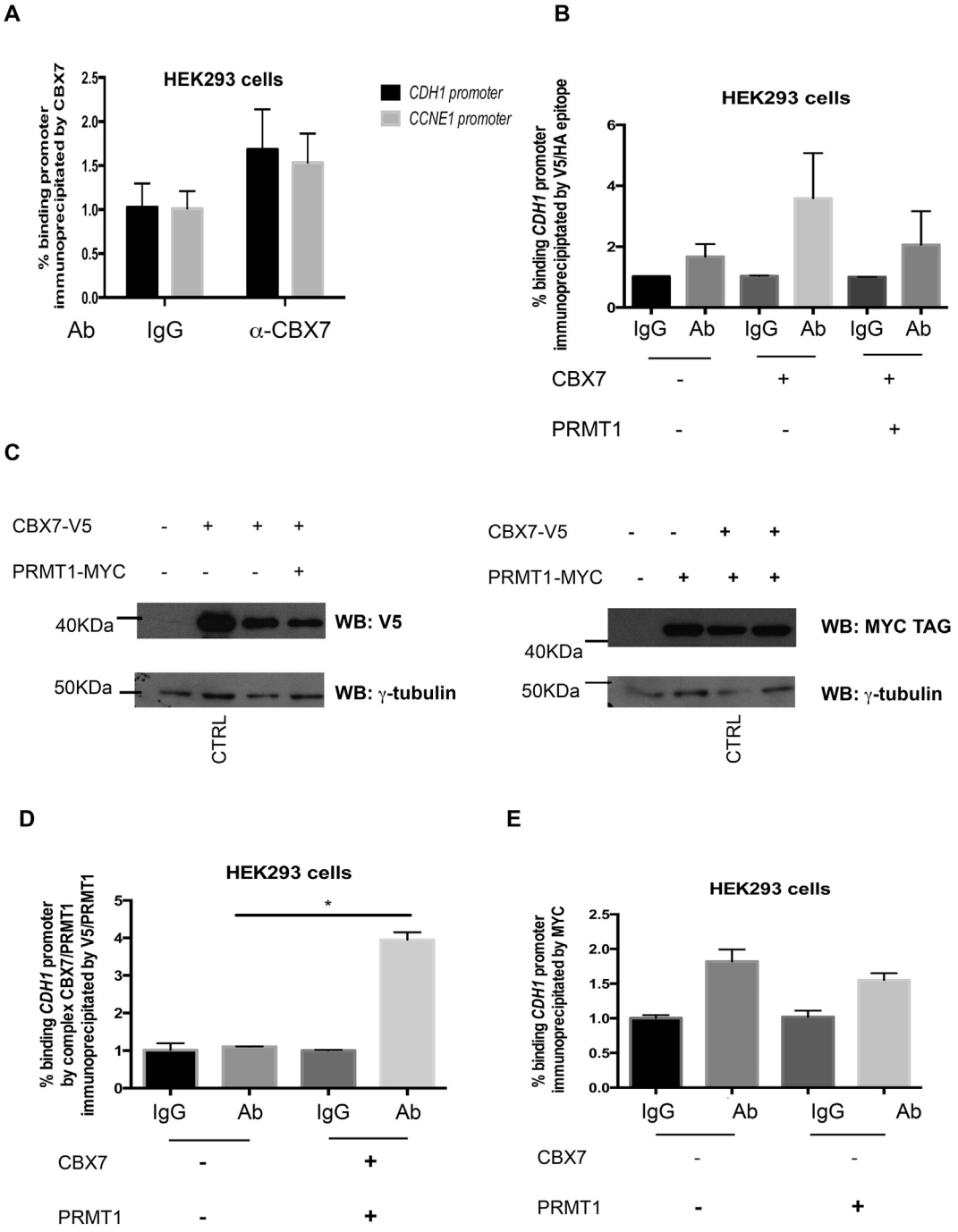

Fig. 2. CBX7 physically interacts with PRMT1 on the *CDH1* promoter. A. HEK293 cells were crosslinked, sonicated and subjected to pre-clearing with IgG. Then, immunocomplexed were immunoprecipitated with IgG and CBX7 antibody. The chomatin was analyzed by qPCR assay performed in triplicate with primers specific for the human *CDH1* and *CCNE* promoters. The sample immunoprecipitated with IgG was set to 1. The shown results represent mean values ± SD of a representative experiment. **B**. HEK293 cells were transiently transfected with either V5-CBX7 and/or MYC-PRMT1 vectors or an empty vector. The chromatin was immunoprecipitated (IP) by using antibodies against V5/HA epitope. The IP chromatin was analyzed by qPCR assay performed in triplicate with primers specific for the human *CDH1* promoter. IgG were used as negative control. The sample immunoprecipitated with IgG was set to 1. The shown results represent mean values ± SEM of five independent experiments. **C.** Immunoblot analysis showing representative samples transfected with V5-CBX7 and MYC-PRMT1. γ-tubulin was used as control to normalize the amount of protein loaded. CTRL: As positive control were used total cellular extracts expressing CBX7 or PRMT1 proteins. **D.** *Re*-chromatin immunoprecipitation experiments in which soluble chromatin immunoprecipitated with anti-V5 antibodies was re-immunoprecipitated with anti-PRMT1. IgG were used as negative control and used to normalize the samples. The sample immunoprecipitated with IgG was set to 1. The shown results are the values of a representative experiment for the human *CDH1* promoter. D'Agostino-Pearson tests were used to evaluate the statistical distribution of samples. Unparaired *t*-test: $^{*}p < 0.05$ **E.** HEK293 cells were transiently transfected with MYC-PRMT1 vectors or an empty vector. The chromatin was immunoprecipitated (IP) by using antibodies against MYC tag epitope. The IP chromatin was analyzed by qPCR assay performed in triplicate with primers specific for the human *CDH1* promoter. IgG were used as negative control and was set to 1. The shown results represent mean values ± SEM of two independent experiments.

interaction on H4R3 dimethylation catalyzed by PRMT1, we evaluated its enzymatic activity in the presence and in the absence of CBX7. The core histone was incubated with recombinant PRMT1 and CBX7 using AdoMet as methyl donor; the same reaction was performed in the absence of CBX7 as a control. Following the methylation reaction, the histone mixture was fractionated by SDS-PAGE and the protein band corresponding to histone H4 was excised from the gel and *in situ* hydrolysed with trypsin under strictly controlled conditions. In these experimental conditions, the enzymatic digestion released tryptic peptides containing several missed cleavages and suitable in size for effective MS and MS/MS analyses. Accordingly, the LC-MS/MS analyses of the corresponding peptide mixtures led to an almost complete mapping of the histone H4 sequence (97% in the presence of CBX7 and 100% in the absence of CBX7). In both these samples the H4 N-terminal sequence (peptide 1–23) was completely mapped revealing both unmodified and differently acetylated peptides, including the N-terminal amino-group, as already observed in a H4 untreated sample.

When only PMRT1 was present in the assay, three peptides were found to map onto the N-terminal region of H4 histone, *i.e.* fragments 1–8, 1–12 and 1–16, all carrying both N-terminal acetylation and Arg3 dimethylation modifications as reported in Table 2. These peptides were, then, selected to evaluate the effect of CBX7 on PRMT1 dimethylation activity. Fig. 3 (A, B) shows the LC-MS chromatograms of dimethylated H4R3 1–8, 1–12 and 1–16 specific peptide ions extracted from the total ion current of tryptic peptides of H4 treated with PRMT1 and AdoMet in the absence (panel A) and in the presence (panel B) of CBX7. The ion current of the unmodified C-terminal peptide 68–77 is reported for normalization. In the presence of CBX7 a decrease in the intensity of the ion current associated to all the H4 dimethylated peptides was clearly observed, demonstrating that the presence of CBX7 results in a inhibition of the PRMT1 methylation activity.

3.4. Effects of CBX7 and PRMT1 on the methylation status of H4R3 in vivo

To investigate the *in vivo* effect of CBX7/PRMT1 binding to the *CDH1* promoter on the methylation status of H4R3, we performed a ChIP assay using antibody specific for the H4R3me2as (asymmetric dimethylation of Histone H4 at Arg3). HEK293 cells were transiently transfected with either individually V5-CBX7 or MYC-PRMT1 or both vectors. The DNA-protein complexes were fixed and then immunoprecipitated by using antibodies against the H4R3me2as. Samples were also immunoprecipitated with aspecific IgG antibodies as a control. Chromatin was released by the immunocomplexes and analyzed by qPCR assay using specific primers for the human *CDH1* promoter. As shown in Fig. 3C, the amount of immunoprecipitated chromatin amplified by qPCR was slightly lower in cells overexpressing CBX7 than in the control, indicating a decrease in dimethylation of H4R3 in the presence of an excess of CBX7. The amount of immunoprecipitated chromatin in cells transfected with MYC-PRMT1 was higher than in the control, indicating an increase of H4R3 dimethylation, as expected.

Finally, when both V5-CBX7 and MYC-PRMT1 were overexpressed, the amount of immunoprecipitated chromatin amplified by qPCR was largely decreased as compared to PMRT1 alone. These results clearly demonstrate that CBX7 decreases the asymmetric methylation status of H4R3 generated by PRMT1 at the *CDH1* promoter accordingly to the results of *in vitro* methylation assays.

Table 2
List of Peptides identified by *in vitro* methylation assay.

m/z observed	M expected	Peptide (start-end)	Peptides sequences including PTMs[a]
408.7391	815.4636	[1–8]	Acetyl-SG(Dimethyl)RGKGGK
586.3500	1170.6854	[1–12]	Acetyl-SG(Dimethyl)RGKGGKGLGK
763.9473	1525.8800	[1–16]	Acetyl-SG(Dimethyl)RG(Acetyl) KGGKGLGKGGAK

[a] Post-translational modifications.

3.5. CBX7 counteracts the negative transcriptional effect of PRMT1 on CDH1 promoter

Next, to analyze the effects of the CBX7/PRMT1 complex on the *CDH1* promoter activity we performed a luciferase assay in the HeLa cells transfected with a vector encoding the luciferase gene under the control of the *CDH1* promoter. HeLa cells were then transfected with either individually HA-CBX7 or MYC-PRMT1 or both vectors. Fig. 4A shows that CBX7 and PRMT1 displayed an opposite behavior in modulating *CDH1* promoter activity. In the presence of CBX7 alone, the luciferase expression was highly increased. On the contrary, PRMT1 clearly exerted a negative transcriptional effect on *CDH1* promoter as luciferase gene expression was significantly decreased by PRMT1 in a dose-dependent manner. However, when both proteins gathered together at the *CDH1* promoter, a partial rescue of the transcriptional activity was obtained strongly depending on the amount of CBX7. These results were confirmed by evaluating luciferase gene expression in samples transfected with increasing dose of PRMT1 where a clear decrease of CDH1 trancriptional activity could be observed according to increasing amount of the methylatransferase (Fig. 4B). Expression of CBX7 and PRMT1 was verified by western blot (Fig. 4C).

These results were also confirmed by evaluating the expression of *CDH1* gene. HEK293 cells were transfected with either individually V5-CBX7 or MYC-PRMT1 or both vectors and the expression of *CDH1* was measured by RT-qPCR assay using specific primers for the human *CDH1* mRNA. According to previous results, *CDH1* expression increased when the cells were transfected with V5-CBX7 alone, while it decreased in the presence of PRMT1 (Fig. 4D). A partial rescue of *CDH1* expression compared to that observed in the presence of PRMT1 alone could be observed when both proteins were present, confirming the effects of the CBX7/PRMT1 complex on the *CDH1* promoter activity.

These results strongly suggest that CBX7 is able to counteract the transcriptional negative effect of PRMT1 on *CDH1* expression.

3.6. Effects of the CBX7/PRMT1 complex on cell migration

Since CBX7 and PRMT1 are involved in the regulation of *CDH1* expression, we investigated whether CBX7 and PRMT1 might affect cell migration ability. Therefore, A549 cells, a human lung carcinoma cell line, stably expressing empty (A549-EV4) or CBX7 (A549-C2 and A549-C8) vectors were transfected with empty (pENTR) or interfering-PRMT1 (shPRMT1) vectors to silence PRMT1 expression [18,44].

The expression of CBX7 was evaluated by RT-qPCR (Fig. 5A) whereas silencing of PRMT1 in A549 clones was monitored by both RT-qPCR and immunoblotting (Fig. 5B, left and right panels). 24 h after transfection, cells were seeded in a transwell and cell migration ability was evaluated after additional 24 h. As shown in Fig. 5C and E, cells expressing CBX7 (A549-C2 and A549-C8) or silenced for PRMT1 (EV4-shPRMT1) alone showed a lower migration rate than the respective control cells (EV4-pENTR), demonstrating that overexpression of CBX7 or silencing of PRMT1 showed the same effect on cell migration rate.

Interestingly, A549-C2 and A549-C8 clones where PRMT1 was silenced (shPRMT1) showed an analogous migration ability in comparison to the respective controls, suggesting that the inhibition effect of CBX7 and the silencing of PRMT1 are not cooperative, as no additive effect could be observed on cell migration rate. These data were validated by the comparable expression of *CDH1* in the same cells, EV4, C2 and C8, transiently transfected with pENTR or shPRMT1 (Fig. 5D). All together these results reinforced the observation that CBX7 is able to counteract the negative effect of PRMT1 on *CDH1* expression and cell migration due to the inhibition of PRMT1 dimethylation activity.

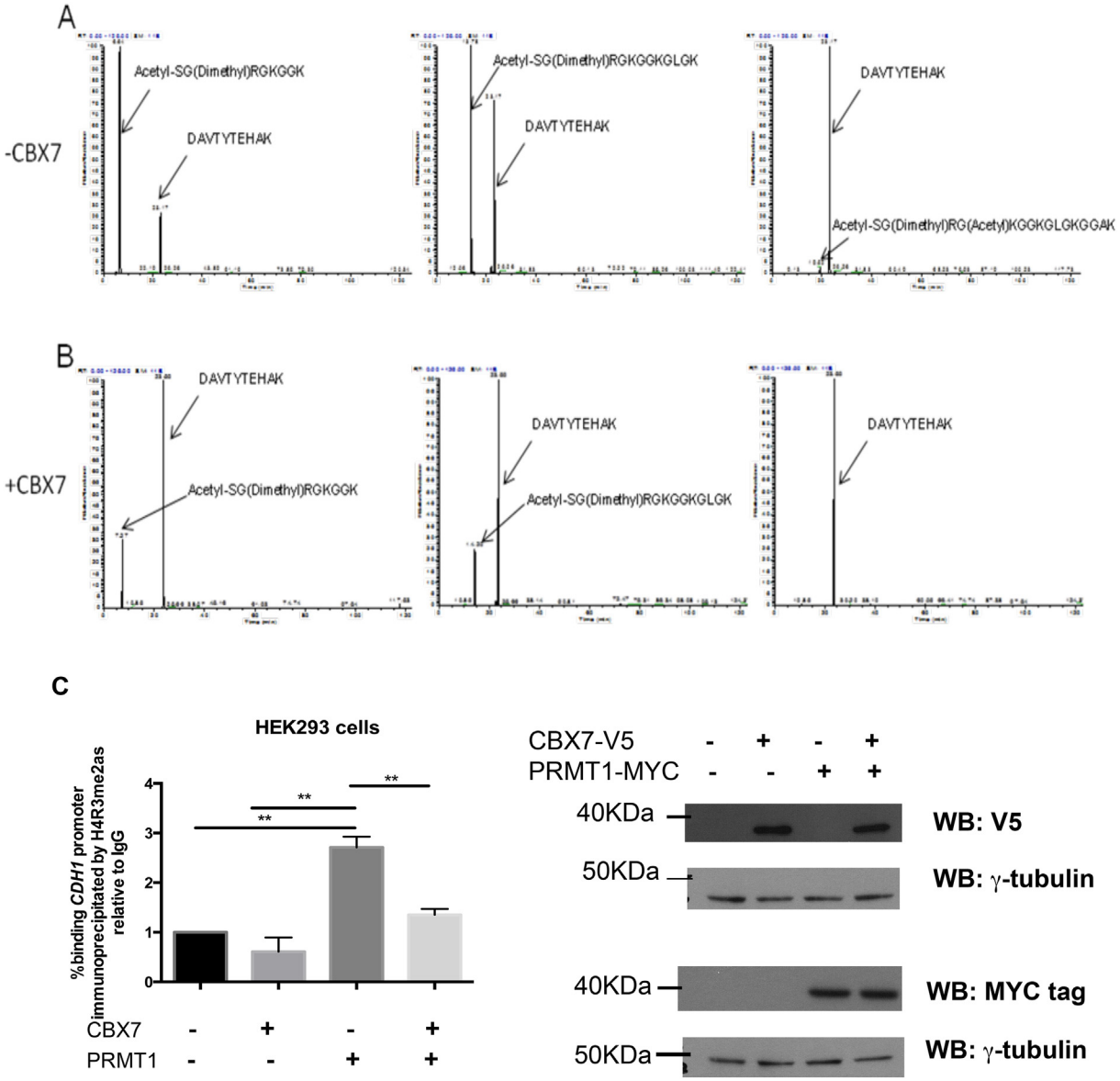

Fig. 3. Effect of CBX7 on the methylation status of H4R3 *in vitro and in vivo*. A, B. Ion extract chromatograms of dimethylated H4R3 1–8, 1–12 and 1–16 peptides from the LC-MS total ion current of tryptic digest of H4 treated with PRMT1 and AdoMet in the absence (Panel A) and in the presence (Panel B) of CBX7. The ion current of the C-terminal peptide 68–77 is also reported for normalization. **C** (left panel) HEK293 cells were transiently transfected with a vector expressing V5-CBX7 protein and/or MYC-PRMT1 protein or with an empty vector. The chromatin was immunoprecipitated (IP) by using antibodies against H4R3me2as and the presence of H4R3 modification was valutated on *CDH1* promoter. IgG were used as negative control. The representation of the value of empty vector (immunoprecipitated by Ab) was set to 1 as medium value of all samples transfected by empty vector. The shown results represent mean values ± SEM of four independent experiments. D'Agostino-Pearson tests were used to evaluate the statistical distribution of samples. Ordinary one-way Anova $^{**}p < 0.01$. (right panel) Immunoblot analysis showing representative samples transfected with V5-CBX7 and MYC-PRMT1. γ-tubulin was used as control to normalize the amount of protein loaded.

4. Discussion

Epigenetic modifications, including those occurring on DNA and histone proteins, control gene expression by establishing and maintaining different chromatin profiles. Arginine methylation is one of several post-translational modifications (PTMs) occurring on histones, catalyzed by a family of PRMTs (protein arginine methyltransferases). This modification is involved in the regulation of the epigenome largely by controlling the recruitment of effector molecules to chromatin. Histone marks have context-dependent functions on transcription and, indeed, arginine methylation associates with both active and repressed chromatin status depending on the residue involved and the configuration of the deposited methyl groups. Histones are susceptible to various PTMs including phosphorylation, methylation, acetylation and ubiquitination whose individual effect on transcription is not univocally assessable [3,39,40]. Numerous histone modifications communicate among themselves by influencing the presence of each other or by collaborating to lead about a functional outcome. Histones can be post-translationally modified to reorganize chromatin in many ways, including already mentioned phosphorylation, ubiquitination, acetylation, and methylation, but also, with different and specific combination of sites, types and extents of histone modifications. In fact, the 'Histone Code Hypothesis' suggests that changed combinations of histone modifications may regulate chromatin structure and transcriptional status, also in a context dependent manner [30,41].

Moreover, cross-talks can occur on the same histone (*cis*) or between different histones (*trans*), and it has been proposed that *trans* mechanisms could even involve more than one nucleosome [42]. The study of

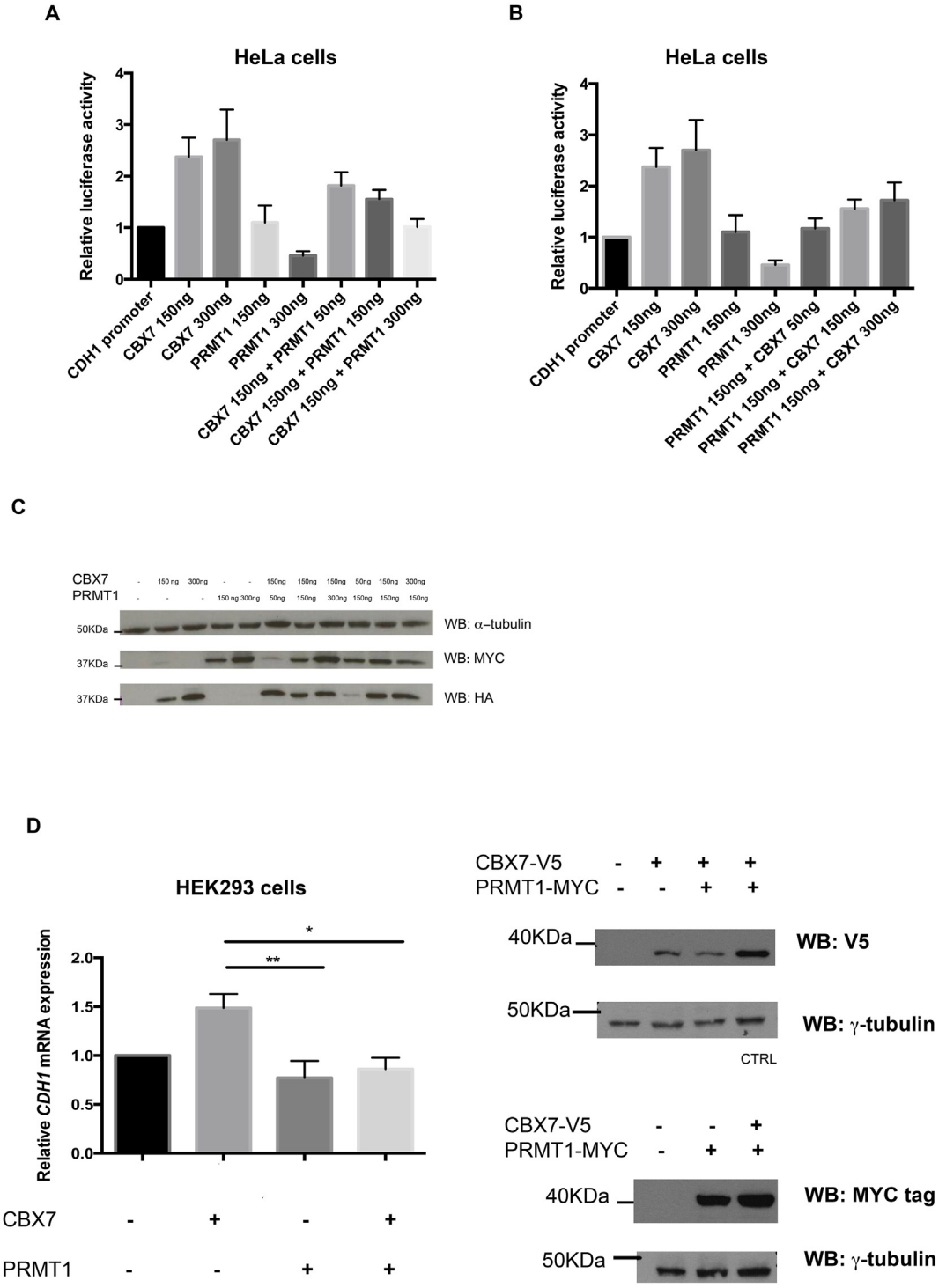

Fig. 4. CBX7 counteracts the negative transcriptional effect of PRMT1 on *CDH1* promoter. A, B. HeLa cells were transfected with the *E-cadherin*-luc vector and with single or both vectors expressing HA-CBX7 or MYC-PRMT1. The double-transfected samples had increasing doses of either HA-CBX7 or MYC-PRMT1 vector. The total amount of the transfected DNA was balanced with the empty vector. Relative Luciferase Activity was calculated relative to that observed in cells transfected with the *E-cadherin*-luc vector and the empty vector alone, assumed equal to 1. Values are the mean of eight independent experiments performed in triplicate ± SEM. **C.** Immunoblot analysis showing representative samples transfected with V5-CBX7 and MYC-PRMT1. α − tubulin was used as control to normalize the amount of protein loaded. **D** (Left panel) HEK293 cells were transfected with single or both vectors encoding V5-CBX7 or MYC-PRMT1. The total amount of the transfected DNA was balanced with the empty vector. Relative *CDH1* mRNA expression represents values normalized to control cells transfected with the only empty vector, that was set equal to 1. Values are the mean of six independent experiments performed in triplicate ± SEM. D'Agostino-Pearson tests were used to evaluate the statistical distribution of samples. Ordinary one-way Anova $*p < 0.05$, $**p < 0.01$. (Right panel) Immunoblot analysis showing representative samples transfected with V5-CBX7 and MYC-PRMT1. γ-tubulin was used as control to normalize the amount of protein loaded. CTRL: positive control expressing CBX7 and PRMT1 proteins.

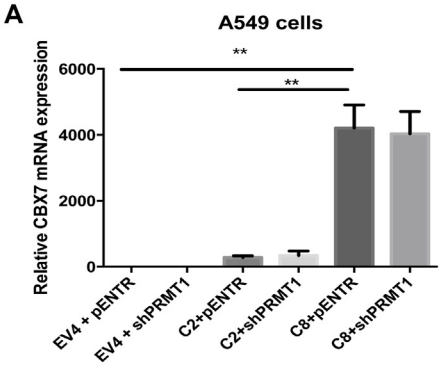

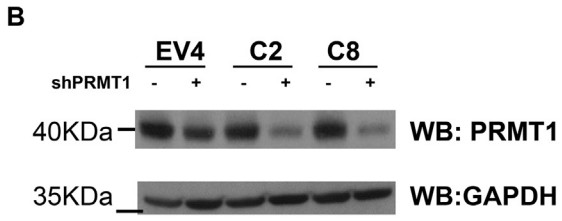

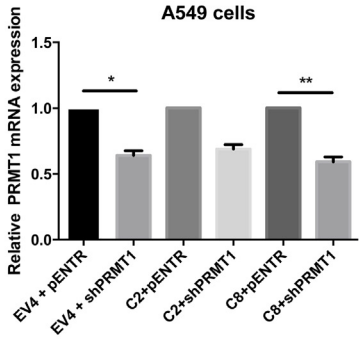

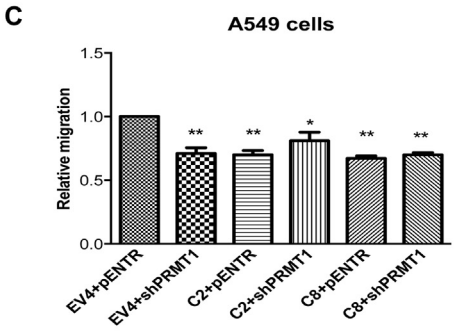

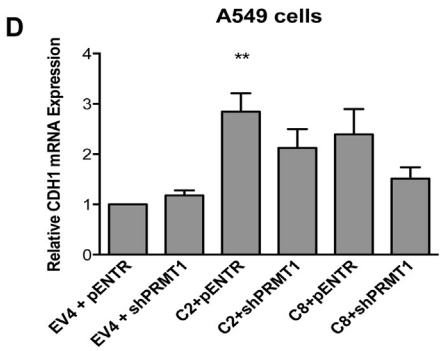

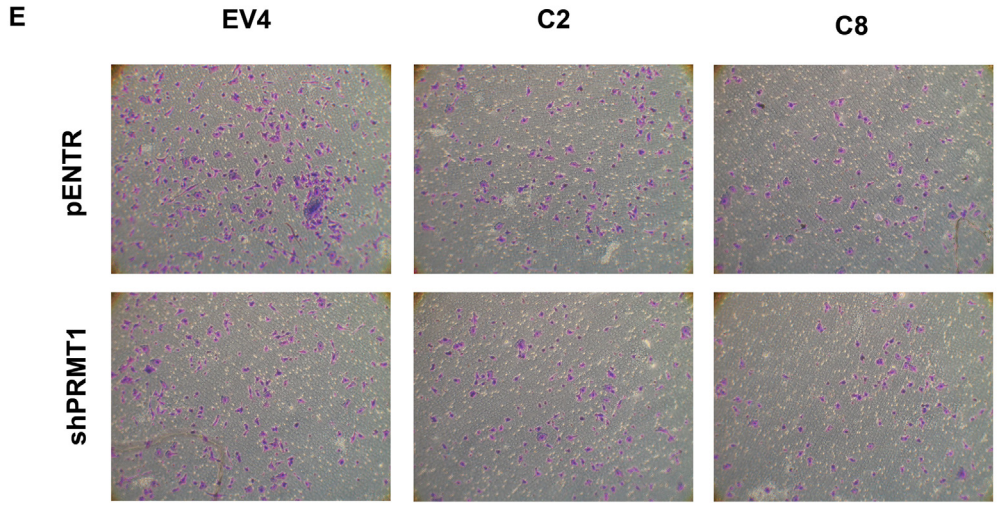

(caption on next page)

Fig. 5. Effects of the CBX7/PRMT1 on cell migration. A. A549 clones (EV4, C2 and C8), transiently transfected with pENTR or shPRMT1, were subjected to RT-qPCR. Relative CBX7 mRNA expression represents values normalized to Empty vector clone (EV4), that was set equal to 1. Values are the mean of two independent experiments performed in triplicate ± SEM. D'Agostino-Pearson tests were used to evaluate the statistical distribution of samples. Ordinary one-way Anova $^{**}p < 0.01$. B. (left panel) A549 clones (EV, C2 and C8) were subjected to RT-qPCR. Relative PRMT1 mRNA expression represents values in cells transfected with shPRMT1 normalized to respective cells transfected with pENTR vector, that was set equal to 1. Values are the mean of four independent experiments performed in triplicate ± SEM. D'Agostino-Pearson tests were used to evaluate the statistical distribution of samples. Kruskal-Wallis test $^{*}p < 0,05$, $^{**}p < 0.01$. (right panel) A representative immunoblot analysis confirming the reduced expression of PRMT1 after transfection with shPRMT1 in A549 clones (EV4, C2 and C8). GAPDH was evaluated to normalize the amount of the protein used. C. A549 clones, stably transfected with empty vector (EV4) and CBX7 (C2 and C8), were re-transfected with empty vector (pENTR) or interfering vector for PRMT1 (shPRMT1) and, then, cells were seeded in a transwell. Transwells were de-stained and cell migration rate was evaluated by monitoring the crystal violet solution at 595 nm/cell tyter of plated cells. Values obtained were normalized with respect to control cells stably transfected with the empty vector whose value was set equal to 1. Values are the mean of three independent experiments performed in triplicate ± SEM. D'Agostino-Pearson tests were used to evaluate the statistical distribution of samples. Ordinary one-way Anova $^{*}p < 0,05$, $^{**}p < 0.01$. D. A549 clones (EV, C2 and C8), transiently transfected with pENTR or shPRMT1 were subjected to RT-qPCR. Relative *CDH1* mRNA expression represents values normalized to Empty vector clone (EV4), that was set equal to 1. Values are the mean of four independent experiments performed in triplicate ± SEM. D'Agostino-Pearson tests were used to evaluate the statistical distribution of samples. Ordinary one-way Anova $^{**}p < 0.01$.E. Transwell pictures from a representative experiment in A549 clones (EV, C2 and C8) transiently transfected with pENTR or shPRMT1. Magnification 40×.

these cross-talks has received great attention because the reading of these modifications by different effectors influences gene expression, and misinterpretation of these cross-talks by readers may trigger various diseases, including cancer [43,44]. All known cross-talk mechanisms described also for arginine methylation on H4 involve Arg3, and specifically its dimethylated (asymmetric or symmetric) forms.

CBX7 is a Polycomb protein that positively or negatively modulates the expression of several genes involved in development and differentiation by recognizing and binding specific histone modification sites on the chromatin structure [1,14]. Several studies have shown that the loss of CBX7 expression correlates with poor prognosis in several cancer tissues [6–13] and, more recently, with chemoresistance to antineoplastic drugs [18] suggesting a critical role of CBX7 in cancer progression.

In order to better define the role and the molecular mechanisms of CBX7 in cancer progression, we designed ChIP/MS-MS assays to identify CBX7 interacting proteins that bind specific DNA regions. Among several identified CBX7 protein partners, we focused our attention on PRMT1 protein that transfers methyl groups from the ubiquitous cofactor S-adenosyl-l-methionine (AdoMet) to the arginine residues of many histone and nuclear/cytoplasmic proteins. The presence of several evidences correlating PRMT1 functions to the control of cell proliferation and to the development and cancer progression has accounted for this choice. Indeed, aberrant expression of PRMT1 has been observed in several cancer tissues [21–26]. More recently, PRMT1 has also been described as an important regulator of EMT acting by repressors of *CDH1* expression [45,46]. EMT is a complex phenomenon and an important driver of tumor invasion, and, then, of metastasis development. A hallmark of EMT is considered the downregulation of *CDH1* that generally reinforces the destabilization of adherent junctions. Since CBX7 positively regulates *CDH1*, we have proposed a pathway in which CBX7 downregulated expression contributes to cancer progression by decreasing *CDH1* expression because of the lack of its inhibitory effect on HDAC2 activity on the *CDH1* promoter [17].

Therefore, aiming to define the biological functions of the CBX7/PRMT1 complex and the molecular mechanisms in cancer progression, we demonstrate the contemporary presence of both proteins on the *CDH1* promoter by ChIP and ReChIP experiments. Moreover, the occurrence of the CBX7/PRMT1 complex on the *CDH1* promoter decreases the methylation capabilities of PRMT1. Both *in vitro* experiments by LC-MS/MS measurement of dimethylated H4 peptides and *in vivo* ChIP assays with H4R3me2a antibodies reveal a lower modification level of H4R3 in presence of CBX7.

The modification of H4R3me2as by PMRT1 and the CBX7/PMRT1 complex was demonstrated to affect transcription. Using luciferase gene reporter assays, we found that PRMT1 is able to reduce the activity of the *CDH1* promoter and that this negative regulation was inhibited by the presence of CBX7 protein in a dose-dependent manner. These results were further confirmed by the analysis of *CDH1* mRNA expression. *CDH1* expression decreased in the presence of PRMT1 but this negative effect was partially rescued in the presence of CBX7.

The ability of PRMT1 to increase H4R3me2as and *CDH1* expression in absence of its binding to *CDH1* promoter is in agreement with previous published data that demonstrate that PRMT1 negative regulates *E-cadherin* transcription through PRMT1-mediated Twist methylation, without an its direct binding on *E-cadherin* promoter [45].

Moreover, it has been demonstrated that the Polycomb proteins can regulate gene transcription in absence of the binding of the enzyme of PRC1 complex to the DNA [3].

Consistently with the biological role of the CBX7-PRMT1 complex, we showed that transfected cells with shPRMT1 displayed a lower migration ability than control cells. The migration rate of thyroid carcinoma cells was analogously decreased in the presence of both CBX7 and PRMT1, confirming previous data on the opposite effects of CBX7 and PRMT1 in the regulation of *CDH1* expression.

5. Conclusions

The overall model (summarized in Fig. 6), suggested by the data reported here, seems to indicate that CBX7 physically interacts with PRMT1, and that this interaction takes place on the *E-cadherin* promoter where CBX7 counteracts the H4R3 dimethylation activity of PRMT1 leading to increased *E-cadherin* mRNA levels. Then, the association between CBX7 and PRMT1 primarily serves to decrease methylation and to increase chromatin association by PRMT1, eventually regulating *E-cadherin* expression and preventing EMT.

Therefore, it can be assumed that a subtle cellular balance exists between CBX7 and histone modification enzymes like HDAC2 and PRMT1. Then, a disruption of this equilibrium, due to a decreased expression of CBX7 in neoplastic tissues, may contribute to cancer progression inducing impairment of *CDH1* expression and increased cell migration eventually leading to EMT.

Disclosure statement

The Authors have nothing to disclose.

Transparency document

The Transparency document associated this article can be found, in online version.

Acknowledgment

We thank Dr. Rama Kamesh Bikkavilli of University of Illinois at Chicago that gently provided us pENTR vector and shPRMT1 construct [45]. We also thank Dr. Tiziana Bonaldi of IEO (Milan) for technical and scientific assistance about CHIP-MS experiment [32,33].

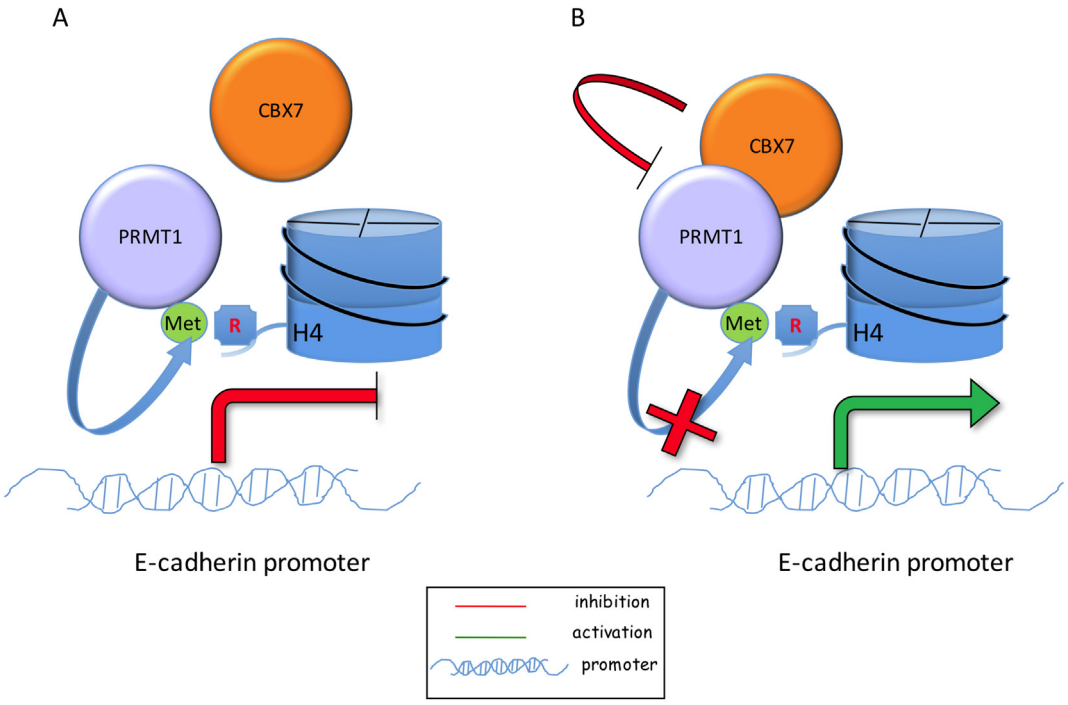

Fig. 6. Model of activity of CBX7-PRMT1 complex on *CDH1* promoter. A. CBX7 and PRMT1 are normally present in cells. **B.** When CBX7 physically interacts with PRMT1, and this interaction takes place on the *E-cadherin* promoter, CBX7 counteracts the H4R3 dimethylation activity of PRMT1 leading to increased *E-cadherin* mRNA levels, through different mechanisms [45,46].

This work was supported by grants provided by: “Progetto di Interesse Strategico Invecchiamento (PNR-CNR Aging Program) PNR-CNR 2012-2014” and “CNR Flagship Projects (Epigenomics-EPIGEN)”. Dr. Romina Sepe was granted with a fellowship provided by “Fondazione Adriano-Buzzati Traverso”, 2016.

Appendix A. Supplementary data

Supplementary data to this article can be found online at https://doi.org/10.1016/j.bbagrm.2019.02.006.

References

[1] A.P. Bracken, K. Helin, Polycomb group proteins: navigators of lineage pathways led astray in cancer, Nat. Rev. Cancer 9 (2009) 773–784, https://doi.org/10.1038/nrc2736.

[2] J.A. Simon, R.E. Kingston, Mechanisms of polycomb gene silencing: knowns and unknowns, Nat. Rev. Mol. Cell Biol. 10 (2009) 697–708, https://doi.org/10.1038/nrm2763.

[3] J.I. Wu, J. Lessard, G.R. Crabtree, Understanding the words of chromatin regulation, Cell 136 (2009) 200–206, https://doi.org/10.1016/j.cell.2009.01.009.

[4] A.H. Lund, M. van Lohuizen, Polycomb complexes and silencing mechanisms, Curr. Opin. Cell Biol. 16 (3) (2004) 239–246, https://doi.org/10.1016/j.ceb.2004.03.010.

[5] S. Aranda, G. Mas, L. Di Croce, Regulation of gene transcription by Polycomb proteins, Sci. Adv. 1 (11) (2015 Dec) e1500737, , https://doi.org/10.1126/sciadv.1500737.

[6] P. Pallante, A. Federico, M.T. Berlingieri, M. Bianco, A. Ferraro, F. Forzati, A. Iaccarino, M. Russo, G.M. Pierantoni, V. Leone, S. Sacchetti, G. Troncone, M. Santoro, A. Fusco, Loss of the CBX7 gene expression correlates with a highly malignant phenotype in thyroid cancer, Cancer Res. 68 (16) (2008 Aug 15) 6770–6778, https://doi.org/10.1016/j.ejca.2010.05.011.

[7] P. Pallante, L. Terracciano, V. Carafa, S. Schneider, I. Zlobec, A. Lugli, M. Bianco, A. Ferraro, S. Sacchetti, G. Troncone, A. Fusco, L. Tornillo, The loss of the CBX7 gene expression represents an adverse prognostic marker for survival of colon carcinoma patients, Eur. J. Cancer 46 (12) (2010 Aug) 2304–2313.

[8] E. Karamitopoulou, P. Pallante, I. Zlobec, L. Tornillo, V. Carafa, T. Schaffner, M. Borner, I. Diamantis, F. Esposito, T. Brunner, A. Zimmermann, A. Federico, L. Terracciano, A. Fusco, Loss of the CBX7 protein expression correlates with a more aggressive phenotype in pancreatic cancer, Eur. J. Cancer 46 (2010) 1438–1444, https://doi.org/10.1016/j.ejca.2010.01.033.

[9] S. Hinz, C. Kempkensteffen, F. Christoph, H. Krause, M. Schrader, M. Schostak, K. Miller, S. Weikert, Expression parameters of the polycomb group proteins BMI1, SUZ12, RING1 and CBX7 in urothelial carcinoma of the bladder and their prognostic relevance, Tumour Biol. 29 (2008) 323–329, https://doi.org/10.1159/000170879.

[10] Z. Jiang, J. Guo, B. Xiao, Y. Miao, R. Huang, D. Li, Y. Zhang, Increased expression of miR-421 in human gastric carcinoma and its clinical association, J. Gastroenterol. 45 (2010) 17–23, https://doi.org/10.1007/s00535-009-0135-6.

[11] F. Forzati, A. Federico, P. Pallante, A. Abbate, F. Esposito, U. Malapelle, R. Sepe, G. Palma, G. Troncone, M. Scarfò, C. Arra, M. Fedele, A. Fusco, CBX7 is a tumor suppressor in mice and humans, J. Clin. Invest. 122 (2012) 612–623, https://doi.org/10.1172/JCI58620.

[12] Yu T., Wu Y., Hu Q., Zhang J., Nie E., Wu W., Wang X., Wang Y., Liu N. CBX7 is a glioma prognostic marker and induces G1/S arrest via the silencing of CCNE1. Oncotarget. 2017 Apr 18;8(16):26637–26647. doi: 10.18632/oncotarget.15789.

[13] G. Mansueto, F. Forzati, A. Ferraro, P. Pallante, M. Bianco, F. Esposito, A. Iaccarino, G. Troncone, A. Fusco, Identification of a new pathway for tumor progression: microRNA-181b up-regulation and CBX7 down-regulation by HMGA1 protein, Genes Cancer 1 (2010) 210–224, https://doi.org/10.1177/1947601910366860.

[14] P. Pallante, F. Forzati, A. Federico, C. Arra, A. Fusco, Polycomb protein family member CBX7 plays a critical role in cancer progression, Am. J. Cancer Res. 5 (5) (2015) 1594–1601.

[15] P. Pallante, R. Sepe, A. Federico, F. Forzati, M. Bianco, A. Fusco, CBX7 modulates the expression of genes critical for Cancer progression, PLoS One 9 (5) (2014) e98295, , https://doi.org/10.1371/journal.pone.0098295.

[16] R. Sepe, U. Formisano, A. Federico, F. Forzati, A.U. Bastos, D. D'Angelo, N.A. Cacciola, A. Fusco, P. Pallante, CBX7 and HMGA1b proteins act in opposite way on the regulation of the SPP1 gene expression, Oncotarget. 6 (5) (2015 Feb) 2680–2692, https://doi.org/10.18632/oncotarget.2777.

[17] A. Federico, P. Pallante, M. Bianco, A. Ferraro, F. Esposito, M. Monti, M. Cozzolino, S. Keller, M. Fedele, V. Leone, G. Troncone, L. Chiariotti, P. Pucci, A. Fusco, Chromobox protein homologue 7 protein, with decreased expression in human carcinomas, positively regulates E-cadherin expression by interacting with the histone deacetylase 2 protein, Cancer Res. 69 (17) (2009 Sep 1) 7079–7087, https://doi.org/10.1158/0008-5472.CAN-09-1542.

[18] N.A. Cacciola, R. Sepe, F. Forzati, A. Federico, S. Pellecchia, U. Malapelle, A. De Stefano, D. Rocco, A. Fusco, P. Pallante, Restoration of CBX7 expression increases the susceptibility of human lung carcinoma cells to irinotecan treatment, Naunyn Schmiedeberg's Arch. Pharmacol. 388 (11) (2015 Nov) 1179–1186, https://doi.org/10.1007/s00210-015-1153-y.

[19] M. Zollo, M. Ahmed, V. Ferrucci, V. Salpietro, F. Asadzadeh, M. Carotenuto, R. Maroofian, A. Al-Amri, R. Singh, I. Scognamiglio, M. Mojarrad, L. Musella, A. Duilio, A. Di Somma, E. Karaca, A. Rajab, A. Al-Khayat, T. Mohan Mohapatra, A. Eslahi, F. Ashrafzadeh, L.E. Rawlins, R. Prasad, R. Gupta, P. Kumari, M. Srivastava, F. Cozzolino, S. Kumar Rai, M. Monti, G.V. Harlalka, M.A. Simpson, P. Rich, F. Al-Salmi, M.A. Patton, B.A. Chioza, S. Efthymiou, F. Granata, G. Di Rosa, S. Wiethoff, E. Borgione, C. Scuderi, K. Mankad, M.G. Hanna, P. Pucci, H. Houlden, J.R. Lupski, A.H. Crosby, Baple E.L. PRUNE is crucial for normal brain development and mutated in microcephaly with neurodevelopmental impairment, Brain. 140 (4)

(2017, Apr 1) 940–952, https://doi.org/10.1093/brain/awx014.
[20] S. Marchiò, M. Soster, S. Cardaci, A. Muratore, A. Bartolini, V. Barone, D. Ribero, M. Monti, P. Bovino, J. Sun, R. Giavazzi, S. Asioli, P. Cassoni, L. Capussotti, P. Pucci, A. Bugatti, M. Rusnati, R. Pasqualini, W. Arap, Bussolino F. A complex of α6 integrin and E-cadherin drives liver metastasis of colorectal cancer cells through hepatic angiopoietin-like 6, EMBO Mol Med. 4 (11) (2012 Nov) 1156–1175, https://doi.org/10.1002/emmm.201101164.
[21] K. Mathioudaki, A. Papadokostopoulou, A. Scorilas, D. Xynopoulos, N. Agnanti, M. Talieri, The PRMT1 gene expression pattern in colon cancer, Br. J. Cancer 99 (12) (2008 Dec 16) 2094–2099, https://doi.org/10.1038/sj.bjc.6604807.
[22] K. Mathioudaki, A. Scorilas, A. Ardavanis, P. Lymberi, E. Tsiambas, M. Devetzi, A. Apostolaki, M. Talieri, Clinical evaluation of PRMT1 gene expression in breast cancer, Tumour Biol. 32 (3) (2011 Jun) 575–582, https://doi.org/10.1007/s13277-010-0153-2.
[23] M. Yoshimatsu, G. Toyokawa, S. Hayami, M. Unoki, T. Tsunoda, H.I. Field, J.D. Kelly, D.E. Neal, Y. Maehara, B.A. Ponder, Y. Nakamura, R. Hamamoto, Dysregulation of PRMT1 and PRMT6, type I arginine methyltransferases, is involved in various types of human cancers, Int. J. Cancer 128 (3) (2011 Feb 1) 562–573, https://doi.org/10.1002/ijc.25366.
[24] C.Y. Chuang, C.P. Chang, Y.J. Lee, W.L. Lin, W.W. Chang, J.S. Wu, Y.W. Cheng, H. Lee, C. Li, PRMT1 expression is elevated in head and neck cancer and inhibition of protein arginine methylation by adenosine dialdehyde or PRMT1 knockdown downregulates proliferation and migration of oral cancer cells, Oncol. Rep. 38 (2) (2017 Aug) 1115–1123, https://doi.org/10.3892/or.2017.5737.
[25] Z. Yu, T. Chen, J. Hébert, E. Li, Richard S. A mouse PRMT1 null allele defines an essential role for arginine methylation in genome maintenance and cell proliferation, Mol. Cell. Biol. 29 (11) (2009 Jun) 2982–2996, https://doi.org/10.1128/MCB.00042-09.
[26] R.M. Baldwin, A. Morettin, J. Côté, Role of PRMTs in cancer: could minor isoforms be leaving a mark? World J. Biol. Chem. 5 (2) (2014 May 26) 115–129, https://doi.org/10.4331/wjbc.v5.i2.115.
[27] S. Jahan, J.R. Davie, Protein arginine methyltransferases (PRMTs): role in chromatin organization, Adv Biol Regul. 57 (2015 Jan) 173–184, https://doi.org/10.1016/j.jbior.2014.09.003.
[28] A. Di Lorenzo, M.T. Bedford, Histone arginine methylation, FEBS Lett. 585 (13) (2011 Jul 7) 2024–2031, https://doi.org/10.1016/j.febslet.2010.11.010.
[29] R.S. Blanc, S. Richard, Arginine methylation: the coming of age, Mol. Cell 65 (1) (2017 Jan 5) 8–24, https://doi.org/10.1016/j.molcel.2016.11.003.
[30] E.L. Greer, Y. Shi, Histone methylation: a dynamic mark in health, disease and inheritance, Nat. Rev. Genet. 13 (2012) 343–357.
[31] K.J. Livak, T.D. Schmittgen, Analysis of relative gene expression data using real-time quantitative PCR and the 2(−Delta Delta C(T)) method, Methods. 25 (4) (2001 Dec) 402–408, https://doi.org/10.1006/meth.2001.1262.
[32] M. Bremang, A. Cuomo, A.M. Agresta, M. Stugiewicz, V. Spadotto, T. Bonaldi, Mass spectrometry-based identification and characterisation of lysine and arginine methylation in the human proteome, Mol. BioSyst. 9 (9) (2013 Sep) 2231–2247, https://doi.org/10.1039/c3mb00009e.
[33] M. Soldi, T. Bonaldi, The ChroP approach combines ChIP and mass spectrometry to dissect locus-specific proteomic landscapes of chromatin. J Vis Exp, 11;(86), DOI (2014 Apr), https://doi.org/10.3791/51220.
[34] M. Caterino, A. Aspesi, E. Pavesi, E. Imperlini, D. Pagnozzi, L. Ingenito, C. Santoro, I. Dianzani, M. Ruoppolo, Analysis of the interactome of ribosomal protein S19 mutants, Proteomics. 14 (20) (2014 Oct) 2286–2296, https://doi.org/10.1002/pmic.201300513.
[35] Marucci A., Cozzolino F, Dimatteo C, Monti M, Pucci P, Trischitta V, Di Paola R. Role of GALNT2 in the modulation of ENPP1 expression, and insulin signaling and action: GALNT2: a novel modulator of insulin signaling. Biochim. Biophys. Acta 2013 Jun; 1833(6):1388–95. doi: https://doi.org/10.1016/j.bbamcr.2013.02.032.
[36] M. Haring, S. Offermann, T. Danker, I. Horst, C. Peterhansel, M. Stam, Chromatin immunoprecipitation: optimization, quantitative analysis and data normalization, Plant Methods 3 (2007 Sep 24) 11, https://doi.org/10.1186/1746-4811-3-11.
[37] X. Zhang, C. Guo, Y. Chen, H.P. Shulha, M.P. Schnetz, T. LaFramboise, C.F. Bartels, S. Markowitz, Z. Weng, P.C. Scacheri, Z. Wang, Epitope tagging of endogenous proteins for genome-wide ChIP-chip studies, Nat. Methods 5 (2) (2008 Feb) 163–165.
[38] J. Vandamme, P. Völkel, C. Rosnoblet, P. Le Faou, P.O. Angrand, Interaction proteomics analysis of polycomb proteins defines distinct PRC1 complexes in mammalian cells, Mol. Cell. Proteomics 10 (4) (2011 Apr) M110.002642.
[39] T. Jenuwein, C.D. Allis, Translating the histone code, Science 293 (2001) 1074–1080, https://doi.org/10.1126/science.1063127.
[40] B.M. Turner, Cellular memory and the histone code, Cell. 111 (2002) 285–291.
[41] E.H. Diane, R. Castro, J. Loscalzo, Epigenetic modifications: basic mechanisms and role in cardiovascular disease, Circulation. 123 (19) (2011 May 17) 2145–2156.
[42] Y. Feng, J. Wang, S. Asher, L. Hoang, C. Guardiani, I. Ivanov, Y.G. Zheng, Histone H4 acetylation differentially modulates arginine methylation by an in Cis mechanism, J. Biol. Chem. 286 (23) (2011 Jun 10) 20323–20334, https://doi.org/10.1074/jbc.M110.207258.
[43] D. Molina-Serrano, V. Schiza, A. Kirmizis, Cross-talk among epigenetic modifications: lessons from histone arginine methylation, Biochem. Soc. Trans. 41 (2013) 751–759, https://doi.org/10.1042/BST20130003.
[44] A. Izzo, R. Schneider, Chatting histone modifications in mammals, Brief Funct Genomics. 9 (5–6) (2010 Dec) 429–443.
[45] S. Avasarala, M. Van Scoyk, M.K. Karuppusamy Rathinam, S. Zerayesus, X. Zhao, W. Zhang, M.R. Pergande, J.A. Borgia, J. DeGregori, J.D. Port, R.A. Winn, R.K. Bikkavilli, PRMT1 is a novel regulator of epithelial-mesenchymal-transition in non-small cell lung cancer, J. Biol. Chem. 290 (21) (2015 May 22) 13479–13489, https://doi.org/10.1074/jbc.M114.636050.
[46] Y. Gao, Y. Zhao, J. Zhang, Y. Lu, X. Liu, P. Geng, B. Huang, Y. Zhang, J. Lu, The dual function of PRMT1 in modulating epithelial-mesenchymal transition and cellular senescence in breast cancer cells through regulation of ZEB1, Sci. Rep. 6 (2016 Jan 27) 19874, , https://doi.org/10.1038/srep19874.